

# QCD parity violation at LHC in warped extra dimension

Naoyuki Haba<sup>1</sup>, Kunio Kaneta<sup>1,2</sup>, and Soshi Tsuno<sup>3</sup>

<sup>1</sup>*Department of Physics, Faculty of Science, Hokkaido University, Sapporo 060-0810, Japan*

<sup>2</sup>*Department of Physics, Osaka University, Toyonaka, Osaka 560-0043, Japan*

<sup>3</sup>*High Energy Accelerator Research Organization (KEK), Tsukuba, Ibaraki 305-0801, Japan*

## Abstract

Extra dimension is one of the most attractive candidates beyond the Standard Model. In warped extra dimensional space-time, not only gauge hierarchy problem but also quark-lepton mass hierarchy can be naturally explained. In this setup, a sizable parity violation through Kaluza-Klein gluon exchange appears in QCD process such as helicity dependent top pair production. We investigate this QCD parity violating process by use of  $SO(5) \times U(1)$  gauge-Higgs unification model. We evaluate LHC observable quantities, i.e., a charge asymmetry and a forward-backward asymmetry of the top pair production, and find that a sizable charge asymmetry can be observed with specific model parameters.

# 1 Introduction

ATLAS and CMS collaborations at the LHC reported a discovery of new boson which is consistent with the Standard Model (SM) Higgs boson [1]. It is important that the observed boson can be really identified to the SM Higgs boson. On the other hand, a stabilization of Higgs self-coupling requires underlying theory behind the SM [2, 3] (see also [4] and references therein). Supersymmetry (SUSY) and extra dimension are most reliable candidates beyond the SM, which naturally contain stable dark matter particles. For warped extra dimension, which is first proposed by Randall and Sundrum (RS) in Ref.[5], provides a framework which solves the hierarchy problem. In the original model, the SM fields are localized to a brane. However, when the SM fermions and gauge bosons propagate in the bulk, models have attractive features such as explaining fermion mass hierarchy (see, for example [6]). In this setup, configuration of the SM fermion wave function depends on bulk mass parameters  $c_i$ , where  $i$  is a label of fermion. Fermions with  $c_i > 1/2$  are localized near the Planck brane, while the ones with  $c_i < 1/2$  are localized near the TeV brane. Since the Higgs is localized to the TeV brane, mass of fermions with  $c_i > 1/2$  is smaller than that of fermions with  $c_i < 1/2$  due to overlap of wave functions among the Higgs and fermions. In general,  $c_i$  of left-handed fermions are not the same as those of right-handed fermions[7]. Focusing attention on QCD sector,  $n$ th Kaluza-Klein (KK) gluon  $G^{(n)}$  is localized to the TeV brane. Therefore overlap between  $G^{(n)}$  and  $q_L$  is different from that between  $G^{(n)}$  and  $q_R$ [8]. This means that parity violation in QCD process is accommodated in warped extra dimension scenario.

Parity violation in QCD process can be measured by using helicity dependent top pair production. Helicity measurement of  $t\bar{t}$  is shown in Ref.[9]. In the SM QCD sector, of course, there is no parity violation in top pair production. The SM background is induced by electroweak interaction[10, 11]. The  $t\bar{t}$  helicity asymmetry is expected to be highly sensitive to new physics. For example, SUSY can also arise sizable  $t\bar{t}$  asymmetry through squark loop diagrams, because  $\tilde{q}_L$  and  $\tilde{q}_R$  have different mass spectrum in general, and  $q_{L(R)}-\tilde{q}_{L(R)}-\tilde{g}$  is chiral interaction[11]. For another QCD parity violating process, quarkonium decay is investigated in Ref. [12]. Comparing to the SUSY models, the warped extra dimension model has much larger QCD parity violation due to an existence of tree level contributions.

In this paper, we investigate the QCD parity violation by use of  $SO(5) \times U(1)$  gauge-Higgs unification model as an example of warped extra dimension scenario with bulk quark configurations. That is, Higgs and  $G^{(n)}$  are localized to the TeV-brane, and  $q_L(q_R)$  is typically located near the Planck (the TeV) brane[13].\* We investigate helicity asymmetry of top pair production. It was also researched in Refs.[8], however, we will evaluate it by use of LHC observables, i.e., a charge asymmetry and a forward-backward asymmetry here. We will find that a sizable charge asymmetry can be observed with specific model parameters.

---

\* In general, configuration of quark wave function is also different among their flavor. Thus a different configuration between  $q_L$  and  $q_R$  induces not only parity violation but also flavor violation. Constraints from flavor violation are studied in Refs.[14].

This paper is organized as follows. In section 2, we give a brief review of  $SO(5) \times U(1)$  gauge-Higgs unification model. In section 3, we analyze the  $t\bar{t}$  left-right asymmetry  $A_{LR}$ , which can be observed by a charge asymmetry  $A_C$ , and a forward-backward asymmetry  $A_{FB}$  in the LHC experiment. We present a conclusion in section 4.

## 2 $SO(5) \times U(1)$ gauge-Higgs unification model

We pick up  $SO(5) \times U(1)$  gauge-Higgs unification model as a warped extra dimension scenario in which Higgs and KK gluon are localized to the TeV brane and left- and right-handed fermions have different configurations in the bulk. The model is constructed in the RS warped space-time [5], which metric is given by

$$ds^2 = e^{-2\sigma(y)} \eta_{\mu\nu} dx^\mu dx^\nu + dy^2, \quad (2.1)$$

where  $\sigma(y) = k|y|$  with 5-dimensional scalar curvature  $k$ . The fifth dimension  $y$  is orbifolded on  $S^1/Z_2$ , and the region of  $y$  is given by  $0 \leq y \leq L$ . The Planck and the TeV brane are located at  $y = 0$  and  $y = L$ , respectively. Gauge group of this model is  $SO(5) \times U(1)_X \times SU(3)_C$  in the bulk, and  $SO(5) \times U(1)_X$  is reduced to  $SU(2)_L \times SU(2)_R \times U(1)_X$  by orbifold boundary conditions. The  $SU(2)_R \times U(1)_X$  symmetry breaks down to  $U(1)_Y$  by vacuum expectation value (VEV) of a scalar field  $\Phi$  on the Planck brane.

At low energy scale, relevant parameters in QCD sector of this model are  $k$ , the warp factor  $z_L = e^{kL}$ , 5D strong gauge coupling  $g_C$ , bulk mass parameters  $c_q$ , and brane mass ratios  $\tilde{\mu}^q/\mu_2^q$ . The  $g_C$  is related to 4D strong gauge coupling as  $g_s = g_C/\sqrt{L}$ . Basically  $c_q$  controls the localization of the zero mode wave functions near the TeV brane and the Planck brane.  $\tilde{\mu}^q$  and  $\mu_2^q$  are induced by VEV of the scalar field  $\Phi$ . Brane mass matrices are regarded as flavor diagonal so that the flavor mixing is turned off in this paper. Our setup follows in Ref. [13], and unknown parameters are  $(k, z_L, c_q, \tilde{\mu}^q/\mu_2^q)$  at low energy. Three of these parameters can be fixed by taking electroweak coupling  $\alpha_W$ ,  $W$  boson mass  $m_W$ , and quark mass  $m_q$ . One parameter of  $(k, z_L, c_q, \tilde{\mu}^q/\mu_2^q)$  remains as a free parameter, and we take  $z_L$  as an input parameter. In this paper we consider two cases of  $z_L = 10^{15}$  and  $z_L = 10^{20}$ . Once the  $z_L$  parameter is fixed, Higgs mass is determined. When we input  $z_L$  as  $z_L = 10^{15}$  and  $10^{20}$ , Higgs mass is calculated as  $m_H = 135$  GeV and 158 GeV when  $\theta_H = \frac{\pi}{2}$ , respectively. This is not compatible with recent experimental data, and the suitable Higgs mass can be obtained when  $\theta_H \neq \frac{\pi}{2}$ . Such  $\theta_H$  might be realized by taking specific matter content, for example, and QCD sector is not affected by such modification of the model. We focus on the QCD sector of this model, and therefore, our analysis is not conflicted with the observed  $m_H$ .

In the  $SO(5) \times U(1)$  gauge-Higgs unification model, parity is violated in QCD process because of difference between  $q_L\text{-}\bar{q}_L\text{-}G^{(n)}$  and  $q_R\text{-}\bar{q}_R\text{-}G^{(n)}$  couplings. As we show in section 3, the latter coupling is much larger than the former one. This is because that  $q_R$  ( $q_L$ ) wave function is located near the TeV (the Planck) brane, and KK gluon is located near the TeV brane. Such

configuration of quark wave function is related to brane mass parameters induced by VEV of  $\Phi$  on the Planck brane. Only left-handed quark has brane mass terms, and mixes with extra particles located on the Planck brane. These chiral interactions induce a sizable parity violation in QCD process, which can be discovered at LHC. In order to investigate this parity violation, we focus on helicity dependence of top pair production at LHC.

### 3 Experimental observables at LHC

#### 3.1 Production cross sections

Firstly we prepare parameter sets of the model. Parity violation in QCD process arises from one KK gluon exchange at tree level, which process is  $q\bar{q} \rightarrow G^{(n)} \rightarrow t\bar{t}$ . KK gluon masses and their total decay widths are shown in Tables 1 (a) with  $z_L = 10^{15}$  and (b) with  $z_L = 10^{20}$ . The couplings of KK gluon to quarks are listed in Table 2, where  $g_q^{G^{(n)}}$  represents  $q\text{-}\bar{q}\text{-}G^{(n)}$  coupling constants in unit  $g_s = g_C/\sqrt{L}$ .  $c_q$  and  $\tilde{\mu}^q/\mu_2^q$  are given in Table 3.

unit GeV	1st KK gluon	2nd KK gluon	3rd KK gluon
mass	1144	2630	4111
$\Gamma_{\text{total}}$	7205	1265	274.3

(a)

unit GeV	1st KK gluon	2nd KK gluon	3rd KK gluon
mass	1330	3030	6452
$\Gamma_{\text{total}}$	10987	1615	175.7

(b)

Table 1: KK gluon masses and their total decay widths,  $\Gamma_{\text{total}}$ , with (a)  $z_L = 10^{15}$  and (b)  $z_L = 10^{20}$ .

The production cross sections of the first, second and third KK gluons with the parameters of  $z_L=10^{15}$  and  $10^{20}$  are summarized in Table 4, where the top quark mass is 172.5 GeV and CTEQ6L PDF [15] is used for proton-proton collision at  $\sqrt{s} = 8$  TeV. For simplicity, the renormalization and factorization scales are fixed at  $m_Z = 90.188$  GeV, which result in the electroweak and strong coupling constants of  $\alpha(m_Z) = 1/132.507$  and  $\alpha_s(m_Z) = 0.1298$ , respectively. The top pair production cross section of the SM prediction under the same condition is 197.6(1) pb.

Figures 1 (a) and (b) present the top quark  $p_T$  spectrum and the  $t\bar{t}$  invariant mass system  $m_{t\bar{t}}$  with the first and second KK gluons at  $z_L=10^{20}$  together with the SM prediction, respectively. Both Figs. 1 (a) and (b) show that the SM contribution is suppressed in high  $p_T$  or  $m_{t\bar{t}}$  regions, and the first KK gluon production process becomes almost dominant. The top pair production cross section is precisely measured within 10% level [16]. Given the fact that the theoretical

unit $g_s$	$n = 1$	$n = 2$	$n = 3$
$g_{u_L}^{G^{(n)}}$	-0.195	0.133	-0.108
$g_{c_L}^{G^{(n)}}$	-0.195	0.133	-0.108
$g_{t_L}^{G^{(n)}}$	0.442	-0.402	0.295
$g_{d_L}^{G^{(n)}}$	-0.195	0.133	-0.108
$g_{s_L}^{G^{(n)}}$	-0.195	0.133	-0.108
$g_{b_L}^{G^{(n)}}$	0.661	-0.370	0.283
$g_{u_R}^{G^{(n)}}$	6.323	2.129	0.734
$g_{c_R}^{G^{(n)}}$	6.044	1.633	0.568
$g_{t_R}^{G^{(n)}}$	5.603	0.949	0.408
$g_{d_R}^{G^{(n)}}$	6.323	2.129	0.734
$g_{s_R}^{G^{(n)}}$	6.044	1.633	0.568
$g_{b_R}^{G^{(n)}}$	5.500	0.832	0.417

(a)

unit $g_s$	$n = 1$	$n = 2$	$n = 3$
$g_{u_L}^{G^{(n)}}$	-0.168	0.114	0.079
$g_{c_L}^{G^{(n)}}$	-0.168	0.114	0.079
$g_{t_L}^{G^{(n)}}$	0.366	-0.367	-0.221
$g_{d_L}^{G^{(n)}}$	-0.168	0.114	0.079
$g_{s_L}^{G^{(n)}}$	-0.168	0.114	0.079
$g_{b_L}^{G^{(n)}}$	0.563	-0.334	-0.213
$g_{u_R}^{G^{(n)}}$	7.158	2.174	0.455
$g_{c_R}^{G^{(n)}}$	6.900	1.733	0.369
$g_{t_R}^{G^{(n)}}$	6.518	1.143	0.250
$g_{d_R}^{G^{(n)}}$	7.158	2.174	0.455
$g_{s_R}^{G^{(n)}}$	6.900	1.733	0.369
$g_{b_R}^{G^{(n)}}$	6.430	1.039	0.234

(b)

Table 2: The coupling constants of  $q\bar{q}G^{(n)}$  with (a)  $z_L = 10^{15}$  and (b)  $z_L = 10^{20}$  in unit  $g_s$ .

	$c_q$			$\tilde{\mu}^q/\mu_2^q$		
$z_L$	$(u, d)$	$(c, s)$	$(t, b)$	$(u, d)$	$(c, s)$	$(t, b)$
$10^{15}$	0.843	0.679	0.432	2.283	0.0889	0.0173
$10^{20}$	0.757	0.634	0.451	2.283	0.0889	0.0172

Table 3: Bulk mass parameters  $c_q$  and brane mass ratios  $\tilde{\mu}^q/\mu_2^q$  with  $z_L = 10^{15}$  and  $z_L = 10^{20}$ .

uncertainty also gives similar uncertainty at NNLO calculation [17], the shown production cross sections in the table are nearly in the border of the experimental uncertainty. The differential cross section measurements [18] as a function of top quark  $p_T$  or  $m_{t\bar{t}}$  will allow to explore a wide range of the parameter space of this model.

unit pb	1st KK gluon	2nd KK gluon	3rd KK gluon
$z_L=10^{15}$	22.61(2)	0.1573(2)	$6.45(1)\times 10^{-6}$
$z_L=10^{20}$	12.67(1)	0.1065(1)	$8.50(1)\times 10^{-8}$

Table 4: Production cross sections of the first, second and third KK-gluons with the parameters of  $z_L=10^{15}$  and  $10^{20}$  in a unit of pb. The top quark mass is 172.5 GeV and CTEQ6L PDF is used for proton-proton collision at  $\sqrt{s} = 8$  TeV. The Standard Model top pair production cross section is 197.6(1) pb under same condition.

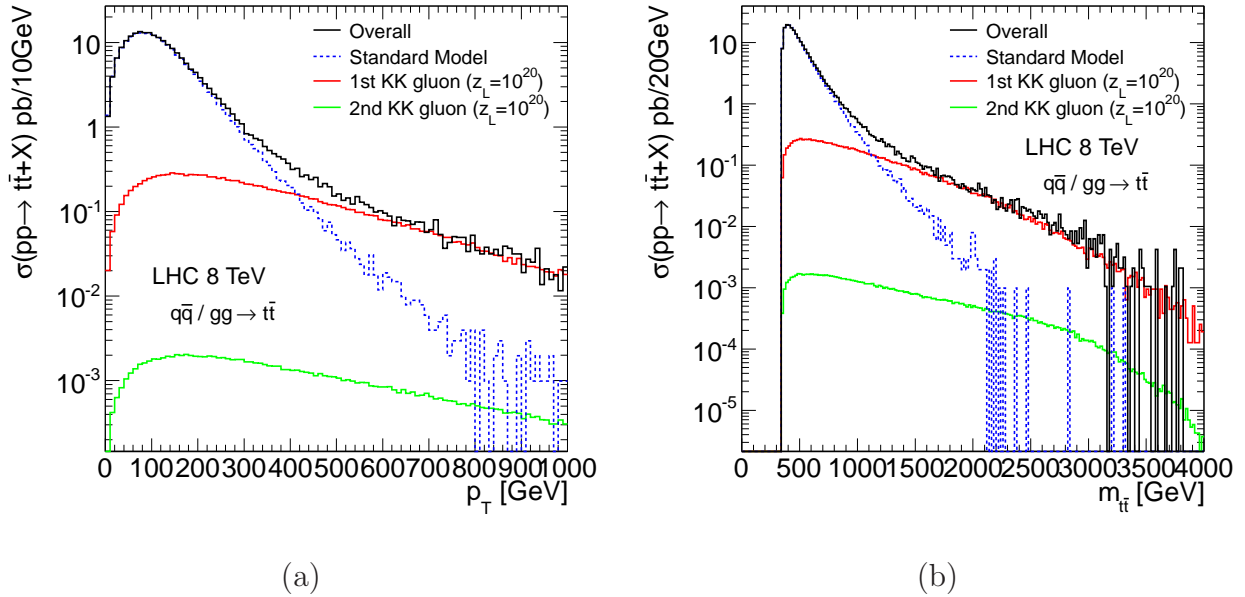


Figure 1: (a) top quark  $p_T$  spectrum and (b)  $t\bar{t}$  invariant mass system  $m_{t\bar{t}}$  with the first and second KK gluons at  $z_L=10^{20}$ .

### 3.2 Asymmetry measurement

Now let us estimate QCD parity violation in the gauge-Higgs unification model. The left-right asymmetry is given as

$$A_{LR} = \frac{N(t_L\bar{t}_L) - N(t_R\bar{t}_R)}{N(t_L\bar{t}_L) + N(t_R\bar{t}_R)} \quad (3.2)$$

where  $N$  is the number of events with left- or right-handed helicity state of the  $t$  ( $t_{L/R}$ ) and  $\bar{t}$  ( $\bar{t}_{L/R}$ ) quarks. First we present the left-right asymmetry  $A_{LR}$  as a function of the  $t\bar{t}$  invariant mass system in Fig. 2. The first, second and third KK gluons are interfered with the SM processes. In the figure, the parameters  $z_L=10^{15}$  and  $10^{20}$  are taken in intuitive purpose. There is a very strong correlation in the asymmetric behavior of the left- and right-handed helicity states of the  $t\bar{t}$  production in the gauge-Higgs unification model, while there is no asymmetric behavior in the SM prediction. This is expected that the KK gluons are strongly coupled with the right-handed top quark. This asymmetric behavior in Fig. 2 can be quantitatively understood as follows. In the high energy limit,  $A_{LR}$  becomes

$$A_{LR} \sim \frac{(g_{t_L}^{G(n)})^2 - (g_{t_R}^{G(n)})^2}{(g_{t_L}^{G(n)})^2 + (g_{t_R}^{G(n)})^2}. \quad (3.3)$$

Thus,  $A_{LR}$  is close to  $-1$  because  $g_{t_L}^{G(n)}$  is much smaller than  $g_{t_R}^{G(n)}$ . Even with the higher order correction, the SM only predicts at most less than 2% [10]. Therefore, the size of the asymmetry might be sufficient to observe in the experiment. Notice again that the helicity state is not identified in the hadron collider experiments, because the  $t$  ( $\bar{t}$ ) quark is not a direct observable. The  $t$  ( $\bar{t}$ ) quark is immediately decayed into the final state particles without suffering the strong interaction, so that the correlation of the helicity state in the  $t\bar{t}$  production is only known through the observation of the final state particle. Since we can not directly know if  $t$  ( $\bar{t}$ ) is left- or right-handed, we should consider the asymmetry of the final state particles ( $t \rightarrow bq\bar{q}/bl\nu$ ). In order to observe the asymmetry in the experiment, we simulate an event close to the experimental conditions. In the rest of this section, we calculate  $t\bar{t}$  asymmetry as charge asymmetry and forward-backward asymmetry defined in Eqs.(3.6) and (3.7), and results are shown in Fig. 3.

The Matrix Element[19] of the top pair productions is considered up to the final state particles involving a decay of the  $t$  ( $\bar{t}$ ) quark, so that the helicity state in the  $t$  ( $\bar{t}$ ) quark in production is properly propagated into the final state particles, and thus the event kinematics could be experimentally modeled. For simplicity, the event selections listed in Table 5 are applied based on the experimental signatures, where the events are categorized as “lepton + jets” and “di-lepton” channels based on the  $W$  boson decay from the  $t$  and  $\bar{t}$  quarks. The lepton + jets

channel	event selection
lepton + jets channel	$p_T > 20 \text{ GeV},  \eta  < 2.5$ for lepton and quarks
di-lepton channel	$p_T > 20 \text{ GeV},  \eta  < 2.5$ for leptons and quarks $\sqrt{\sum_{\nu, \bar{\nu}} p_x^2 + \sum_{\nu, \bar{\nu}} p_y^2} > 50 \text{ GeV}$ for neutrinos

Table 5: Event selections, which categorized as “lepton + jets” and “di-lepton” channels based on the  $W$  boson decay from the  $t$  and  $\bar{t}$  quarks.

channel requires at least one high  $p_T$  electron or muon in the fiducial volume in the detector.

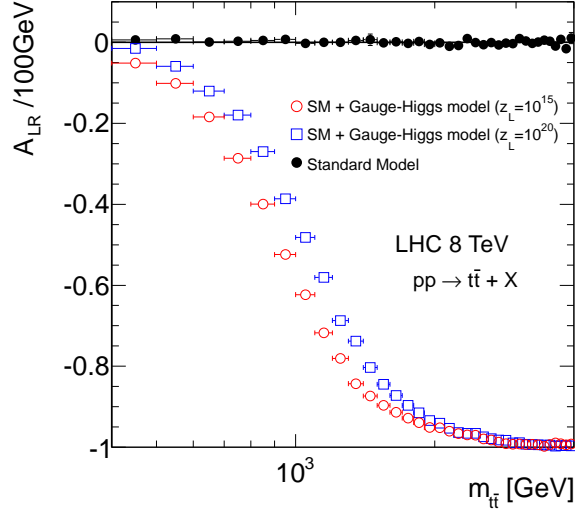


Figure 2: Left-right asymmetry,  $A_{LR}$ , as a function of the  $t\bar{t}$  invariant mass system.

The  $|\eta| < 2.5$  is chosen by the coverage of typical tracking detectors. The  $b$ -quark and the other quarks from  $W$  boson decay are considered as a jet which has to be  $p_T$  larger than 20 GeV with in  $|\eta| < 2.5$ . The  $b$ -jet tagging might enhance the top pair events against background processes. In the di-lepton channel, two leptons ( $e$  or  $\mu$ ) are required in the final state. To further suppress the SM background processes, the missing transverse energy, which is the vectored summation of two neutrino momenta in the transverse plane, is required to be larger than 50 GeV. In the experiment, the un-folding procedure is applied to the observed experimental quantities, and here we only evaluate the 4-vector level event topology to see if given event selections are still feasible to observe the  $t\bar{t}$  asymmetry to probe this model.

Based on these event selections, we define the quantities of the  $t\bar{t}$  asymmetry as follows,

$$A_C = \frac{N(\Delta|y| > 0) - N(\Delta|y| < 0)}{N(\Delta|y| > 0) + N(\Delta|y| < 0)}, \quad \Delta|y| \equiv |y_t| - |y_{\bar{t}}| \quad (3.4)$$

for lepton + jets channel, and

$$A_{FB} = \frac{|\cos \theta_{lep}^+| - |\cos \theta_{lep}^-|}{|\cos \theta_{lep}^+| + |\cos \theta_{lep}^-|} \quad (3.5)$$

for di-lepton channel, respectively. The  $A_C$  is known as the charge asymmetry and  $A_{FB}$  is the forward-backward asymmetry. The  $A_C$  is the difference of the events with the  $t$  ( $\bar{t}$ ) quark rapidities, which is parametrized by  $\Delta|y|$ . The  $t$  ( $\bar{t}$ ) quark direction is reconstructed by three jets from the  $t$  ( $\bar{t}$ ) quark decay. In the di-lepton channel,  $t$  ( $\bar{t}$ ) quark momentum can not be determined. Meanwhile, it is easy to see the charged lepton momentum, and charged leptons in the final state are expected to maintain the asymmetry of  $t$  and  $\bar{t}$  direction. Note that  $A_{FB}$



of (3.5) is not the same observable at the Tevatron because an absolute value of  $t$  ( $\bar{t}$ ) flight direction is meaningful at the LHC.  $A_{FB}$  is formed by the event-by-event basis with the positive and negative charged lepton direction.

Figure 3 (a) shows the charge asymmetry and (b) does forward-backward asymmetry as a function of the invariant mass of the  $t\bar{t}$  system, and di-lepton mass system after event selections applied for lepton + jets and di-lepton channels, respectively. We demonstrate the asymmetries when the gauge-Higgs unification model is included in the SM processes. We also estimate that the integrated  $A_C$  is  $-0.04$ . As for  $A_{FB}$ , it reaches  $-0.1$  in high  $m_{ll}$  region. With 5-10% asymmetry, this is experimentally still sufficient to observe [18].

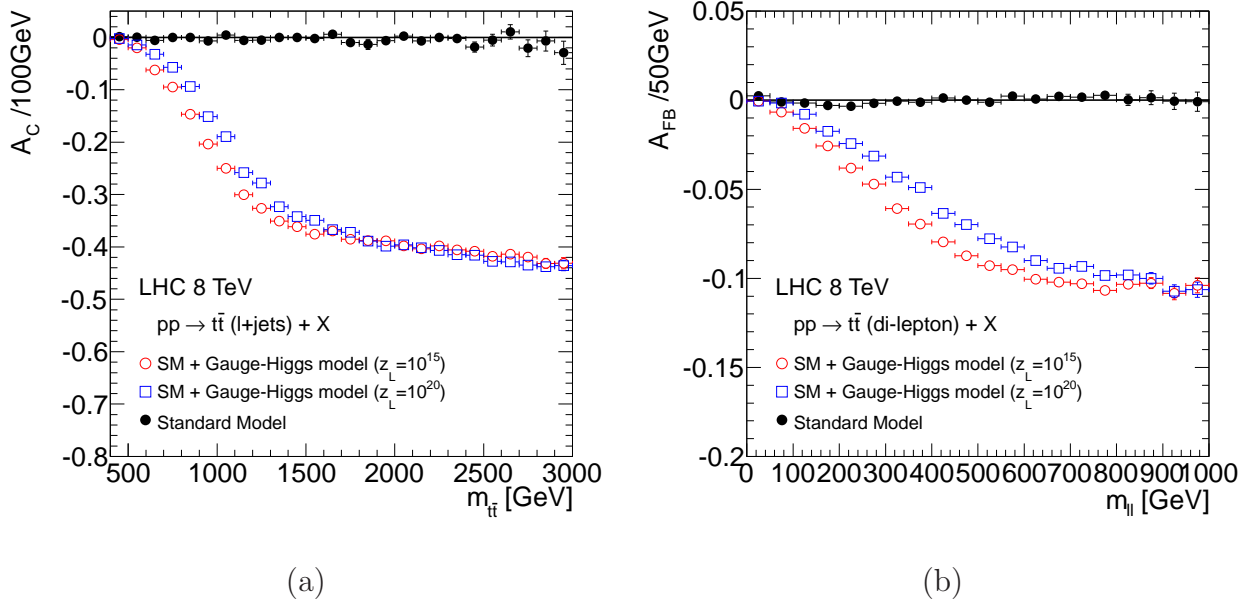


Figure 3: (a) charge asymmetry and (b) forward-backward asymmetry as a function of the invariant mass of the  $t\bar{t}$  system, after event selections applied for lepton + jets and di-lepton channels, respectively.

## 4 Conclusion

We have discussed the parity violation in QCD in warped extra dimension model where Higgs and KK gluon are localized on the TeV brane and left- and right-handed fermions have different configurations in the bulk. In this setup, parity is violated in QCD sector at tree level, which can be observed by the helicity asymmetry of  $t\bar{t}$  at LHC. We pick up  $SO(5) \times U(1)$  gauge-Higgs unification model as a concrete model, and find that large helicity asymmetry appears at high  $m_{t\bar{t}}$  region. We have evaluated LHC observable quantities,  $A_C$  and  $A_{FB}$ , which can reach  $-0.4$

and  $-0.1$ , respectively, with specific parameters in high energy region. We have also estimated the integrated  $A_C$  at  $-0.04$  for all  $m_{t\bar{t}}$  region. Clearly, it is larger than the SM background, and it is sufficient to be experimentally observed. Furthermore, note that the threshold behavior of the asymmetry in the  $t\bar{t}$  invariant mass system is proportional to the first KK gluon mass, and also the saturation behavior of the asymmetry is sensitive to the  $z_L$  parameter.

In the experimental side,  $A_{FB}$  is not yet reported at the LHC. However, it is important because di-lepton channel is expected to be a probe of the  $t\bar{t}$  asymmetry as we discussed in Section 3.2. As for  $A_C$  measurement, statistics is not sufficient in  $m_{t\bar{t}} > 450$  GeV region. Thus, in this region, only an integrated  $A_C$  is reported. The measured charge asymmetry  $A_C$  is consistent with our calculation [20], however, total error (statistic and systematic) is still large ( $\sim 5\%$ ). Statistic and systematic errors are approximately  $\pm 0.03(\text{stat})$  and  $\pm 0.02(\text{syst})$ , respectively. It is necessary to distinguish the KK gluon contribution from the SM background. The SM prediction of  $A_C$  is given by  $A_C^{SM} = 0.00115 \pm 0.0006$  [21]. Then we can recognize the asymmetry to be KK gluon contribution when errors are suppressed as  $\sim 0.01$ . In order to obtain  $\sim 0.01$  statistic error, the integrated luminosity need to be  $\sim 100 \text{ fb}^{-1}$ . While, if the systematic error reduces about  $1/10$ , it is possible to distinguish the  $A_C$  evaluated in this paper from the SM background. Therefore,  $A_C$  is a promising observable for the KK gluon contribution.  $A_{FB}$  is also hopeful observable in di-lepton channel, and the precise measurements of  $A_C$  and  $A_{FB}$  at LHC are important to determine the coupling structure of this model.

## Acknowledgments

We thank Y. Hosotani for helpful discussions. This work is partially supported by Scientific Grant by Ministry of Education and Science, Nos. 22011005, 24540272, 20244028, and 21244036. The works of K.K. are supported by Research Fellowships of the Japan Society for the Promotion of Science for Young Scientists.

## References

- [1] G. Aad *et al.* [ATLAS Collaboration], Phys. Lett. B **716** (2012) 1 [arXiv:1207.7214 [hep-ex]]; S. Chatrchyan *et al.* [CMS Collaboration], Phys. Lett. B **716** (2012) 30 [arXiv:1207.7235 [hep-ex]].
- [2] N. Cabibbo, L. Maiani, G. Parisi and R. Petronzio, Nucl. Phys. B **158**, 295 (1979).
- [3] J. Elias-Miro, J. R. Espinosa, G. F. Giudice, G. Isidori, A. Riotto and A. Strumia, Phys. Lett. B **709**, 222 (2012) [arXiv:1112.3022 [hep-ph]].
- [4] A. Djouadi, Phys. Rept. **457**, 1 (2008) [hep-ph/0503172].
- [5] L. Randall, R. Sundrum, Phys. Rev. Lett. **83** (1999) 3370-3373. [hep-ph/9905221].

- [6] Y. Grossman and M. Neubert, Phys. Lett. B **474** (2000) 361 [hep-ph/9912408]; T. Gherghetta and A. Pomarol, Nucl. Phys. B **586** (2000) 141 [hep-ph/0003129]; S. Chang, C. S. Kim and M. Yamaguchi, Phys. Rev. D **73** (2006) 033002 [hep-ph/0511099]; M. E. Albrecht, M. Blanke, A. J. Buras, B. Duling and K. Gemmler, JHEP **0909** (2009) 064 [arXiv:0903.2415 [hep-ph]].
- [7] S. J. Huber, Nucl. Phys. B **666** (2003) 269 [hep-ph/0303183]; K. Agashe, G. Perez and A. Soni, Phys. Rev. D **71** (2005) 016002 [hep-ph/0408134]; M. S. Carena, A. Delgado, E. Ponton, T. M. P. Tait and C. E. M. Wagner, Phys. Rev. D **71** (2005) 015010 [hep-ph/0410344]; E. De Pree and M. Sher, Phys. Rev. D **73** (2006) 095006 [hep-ph/0603105]; M. S. Carena, E. Ponton, J. Santiago and C. E. M. Wagner, Nucl. Phys. B **759** (2006) 202 [hep-ph/0607106]; G. Cacciapaglia, C. Csaki, J. Galloway, G. Marandella, J. Terning and A. Weiler, JHEP **0804** (2008) 006 [arXiv:0709.1714 [hep-ph]]; C. Csaki, A. Falkowski and A. Weiler, Phys. Rev. D **80** (2009) 016001 [arXiv:0806.3757 [hep-ph]]; S. Casagrande, F. Goertz, U. Haisch, M. Neubert and T. Pfoh, JHEP **0810** (2008) 094 [arXiv:0807.4937 [hep-ph]]; M. E. Albrecht, M. Blanke, A. J. Buras, B. Duling and K. Gemmler, JHEP **0909** (2009) 064 [arXiv:0903.2415 [hep-ph]]; M. Bauer, F. Goertz, U. Haisch, T. Pfoh and S. Westhoff, JHEP **1011** (2010) 039 [arXiv:1008.0742 [hep-ph]].
- [8] B. Lillie, L. Randall and L. -T. Wang, JHEP **0709** (2007) 074 [hep-ph/0701166]; B. Lillie, J. Shu and T. M. P. Tait, Phys. Rev. D **76** (2007) 115016 [arXiv:0706.3960 [hep-ph]]; A. Djouadi, G. Moreau and R. K. Singh, Nucl. Phys. B **797** (2008) 1 [arXiv:0706.4191 [hep-ph]].
- [9] T. Stelzer, S. Willenbrock, Phys. Lett. **B374** (1996) 169-172. [hep-ph/9512292]; M. Beneke, I. Efthymiopoulos, M. L. Mangano, J. Womersley, A. Ahmadov, G. Azuelos, U. Baur, A. Belyaev *et al.*, [hep-ph/0003033]; W. Bernreuther, A. Brandenburg, Z. G. Si and P. Uwer, Phys. Rev. Lett. **87** (2001) 242002 [arXiv:hep-ph/0107086]; W. Bernreuther, A. Brandenburg, Z. G. Si and P. Uwer, Nucl. Phys. B **690** (2004) 81 [arXiv:hep-ph/0403035]; W. Bernreuther, M. Fucker, Z. -G. Si, Phys. Rev. **D74** (2006) 113005. [hep-ph/0610334]. W. Bernreuther, J. Phys. G **G35** (2008) 083001. [arXiv:0805.1333 [hep-ph]].
- [10] W. Beenakker, A. Denner, W. Hollik, R. Mertig, T. Sack, D. Wackeroth, Nucl. Phys. **B411** (1994) 343-380; C. Kao and D. Wackeroth, Phys. Rev. D **61** (2000) 055009 [arXiv:hep-ph/9902202]; W. Bernreuther, M. Fucker and Z. G. Si, Phys. Rev. D **78** (2008) 017503 [arXiv:0804.1237 [hep-ph]].
- [11] N. Haba, K. Kaneta, S. Matsumoto, T. Nabeshima and S. Tsuno, Phys. Rev. D **85** (2012) 014007 [arXiv:1109.5082 [hep-ph]].
- [12] N. Haba, K. Kaneta and T. Onogi, arXiv:1109.5442 [hep-ph].

- [13] Y. Hosotani, M. Tanaka and N. Uekusa, Phys. Rev. D **84** (2011) 075014 [arXiv:1103.6076 [hep-ph]].
- [14] M. Blanke, A. J. Buras, B. Duling, S. Gori and A. Weiler, JHEP **0903** (2009) 001 [arXiv:0809.1073 [hep-ph]]; A. J. Buras, PoS KAON **09** (2009) 045 [arXiv:0909.3206 [hep-ph]].
- [15] J. Pumplin, D. R. Stump, J. Huston, H. L. Lai, P. M. Nadolsky and W. K. Tung, JHEP **0207** (2002) 012 [hep-ph/0201195].
- [16] V. Khachatryan *et al.* [CMS Collaboration], Phys. Lett. B **695** (2011) 424 [arXiv:1010.5994 [hep-ex]]; G. Aad *et al.* [ATLAS Collaboration], Phys. Lett. B **717** (2012) 89 [arXiv:1205.2067 [hep-ex]].
- [17] N. Kidonakis, arXiv:1205.3453 [hep-ph].
- [18] P. Silva *et al.* [ATLAS and CMS Collaborations], arXiv:1206.2967 [hep-ex].
- [19] S. Tsuno, T. Kaneko, Y. Kurihara, S. Odaka and K. Kato, Comput. Phys. Commun. **175** (2006) 665 [hep-ph/0602213].
- [20] S. Chatrchyan *et al.* [CMS Collaboration], Phys. Lett. B **717** (2012) 129 [arXiv:1207.0065 [hep-ex]]; G. Aad *et al.* [ATLAS Collaboration], Eur. Phys. J. C **72** (2012) 2039 [arXiv:1203.4211 [hep-ex]].
- [21] J. H. Kuhn and G. Rodrigo, JHEP **1201** (2012) 063 [arXiv:1109.6830 [hep-ph]].